

Acute exposure to 27.12 MHz radiofrequency electromagnetic field disrupts blood-brain barrier integrity via eNOS activation and occludin down-regulation

Arzu Ulusoy 1*, Halil Asci 1, 2, Rumeysa Taner 1, Muhammet Yusuf Tepebasi 3, Ilter Ilhan 4, Pinar Karabacak 5, Selcuk Comlekci 1, 6, Ozlem Ozmen 7

- Department of Bioengineering, Institute of Natural and Applied Sciences, Suleyman Demirel University, Isparta, Türkiye
- ² Department of Pharmacology, Faculty of Medicine, Suleyman Demirel University, Isparta, Türkiye
- ³ Department of Genetics, Faculty of Medicine, Suleyman Demirel University, Isparta, Türkiye
- ⁴ Department of Biochemistry, Faculty of Medicine, Suleyman Demirel University, Isparta, Türkiye
- ⁵ Department of Anesthesia and Reanimation, Faculty of Medicine, Suleyman Demirel University, Isparta, 1 "rkiye
- ⁶ Department of Electrical and Electronic Engineering, Suleyman Demirel University, Isparta, Türkiye
- ⁷ Department of Pathology, Faculty of Veterinary Medicine, Burdur Mehmet Akif Ersoy University, Burdur, Türkiy

ARTICLE INFO

Article type: Original

Article history: Received: Mar 23, 2025 Accepted: Jul 22, 2025

Keywords:

Blood-Brain Barrier CD31 Claudin-1 eNOS Haptoglobin Occludin Radiofrequencyelectromagnetic fields

ABSTRACT

Objective(s): Controlled modulation of blood-brain ba rier (i BB) permeability without inducing damage represents a promising strategy for enhancing central pervous system drug delivery.

Materials and Methods: This study inversign done effects of 27.12 MHz radiofrequency electromagnetic field (RF-EMF) exposure in 30 180, and 360 min on BBB integrity in female Wistar rats (n=6 per group). Brain and combellar tissues were analyzed histologically and immunohistochemically (haptoglobin CD31), and molecular analyses were performed for oxidative stress parameters (TAS, TOS, and OS inflammatory and hypoxia markers (IL-6 and HIF-1α), endothelial nitric oxide synthase (eNCS), and tight junction proteins (claudin-1 and occludin).

Results: RF-EMF exposure for 30 min sunificantly increased eNOS gene expression without triggering oxidative stress or inflammation. Longer exposures (180 and 360 min) resulted in increased HIF-1 α expression, decreased levels of cloudin 1 and occludin, and histopathological signs of hyperemia and edema, particularly in the cerebellar assue. Notably, occludin expression decreased in all exposure groups, while eNOS was maxim. "y up-regulated at 30 min.

Conclusion: Thirty-minu a RF- MF exposure at 27.12 MHz transiently modulates BBB permeability via eNOS activation and concludin down-regulation without apparent tissue damage. These findings suggest that short-cam PF-EMF application may serve as a non-invasive tool for targeted BBB modulation. Fruther takes are warranted to refine exposure parameters and assess translational potential in the parameters are parameters and assess translational potential in the parameters are parameters and assess translational potential in the parameters are parameters and assess translational potential in the parameters are parameters and assess translational potential in the parameters are parameters and assess translational potential in the parameters are parameters and assess translational potential in the parameters are parameters and assess translational potential in the parameters are parameters are parameters and assess translational potential in the parameters are parameters and assess translational parameters are parameters and parameters are parameters are parameters are parameters and parameters are parameters are parameters and parameters are parameters are parameters and parameters are parameters are parameters are parameters are parameters and parameters are par

► Please cite this article as:

Ulusoy A, Asci H, Taner R, Tepel asi MY, Ilh n I, Karabacak P, Comlekci S, Ozmen O. Acute exposure to 27.12 MHz radiofrequency electromagnetic field disrupts blood-brail barrier integrity via eNOS activation and occludin down-regulation. Iran J Basic Med Sci 2025; 28:

Introduction

The blood-brain barrier (BBB) is a dynamic interface that protects the central nervous system by regulating the passage of substances between the bloodstream and brain parenchyma. While it restricts harmful molecules, it also limits therapeutic drug access to brain tissues, posing a significant obstacle in treating neurological diseases (1, 2).

Modulating BBB permeability in a controlled, reversible, and non-damaging manner is of high clinical interest. Such modulation could allow for enhanced delivery of drugs, including anesthetics, at lower doses, potentially reducing systemic side effects (3, 4). The integrity of the BBB is tightly maintained by tight junction proteins such as occludin and claudins, as well as metabolic enzymes and transporters. Disruption of these structures is often associated with

neuroinflammation and oxidative stress (5, 6).

The passage of substances through the BBB is tightly controlled both physically by tight junctions (TJs) and metabolically by a barrier formed by various enzymes (6). It is known that the permeability of the BBB increases with decreased levels of structures such as claudin-5, occludin-1, and zonulin-1, which provide information about the state of the TJ. Studies are showing that this permeability may also increase in various inflammatory events due to damage (5, 6).

Haptoglobin, an acute-phase response protein, neutralizes hemoglobin in the bloodstream and defends neurons from damage induced by hemolytic products (7). Platelet endothelial cell adhesion molecule-1 (PECAM-1; CD31) regulates vascular repair mechanisms to restore BBB

*Corresponding author: Arzu Ulusoy. Department of Bioengineering, Institute of Natural and Applied Sciences, Suleyman Demirel University, Isparta, Türkiye. Tel/ Fax: +90-544 4782858, Email: arzuulusoy32@gmail.com





integrity (8, 9).

Increased levels of interleukin-6 (IL-6), which is also an acute phase reactant, and increased expression of hypoxia-inducible factor-1 alpha (HIF-1 α) in the presence of hypoxia, regulate inflammatory responses and increase BBB permeability by increasing eNOS-mediated NO synthesis (10, 11).

In a review study examining the effect of NO on BBB integrity, Thiel and Audus (2001) stated that since the BBB is composed of endothelial cells lining the capillaries of the brain, NO will cause the BBB to open under many conditions, including NO-mediated transients in the transmission of substances, which may eventually cause vasogenic edema and secondary brain damage (12).

Radiofrequency electromagnetic field (RF-EMF) is a non-invasive, non-contact adjunctive therapy that involves the delivery of an RF-EMF to a target tissue without direct electrode contact with the body, using a carrier frequency of 27.12 MHz, the medical frequency set by the Federal Communications Commission (13). Bragin *et al.* (2015) demonstrated that a 30-minute RF-EMF exposure at 27.12 MHz increased cerebral arteriolar dilation and NO release, suggesting a vasogenic effect without tissue injury (14). In a recent preliminary study, Taner *et al.* (2023) observed synergistic effects of RF and pulsed magnetic fields on ischemia-reperfusion-induced brain injury, with enhanced perfusion and reduced infarct size (15).

In this study, the effect of 27.12 MHz RF-EMF applied to experimental animals for different durations on the BBB and the NO connection was investigated.

Materials and Methods

Animals and ethical approval

All the experimental procedures were performed under the guidelines of the Animal Research: Reperiments (ARRIVE) guidelines 2.0 and were approved by the Committee on Animal Research of Suley man Demirel University, Isparta (Approval No: 26.2.2023/01-129). Twenty-four adult Wistar Albin female rats, weighing 300-350 g, were obtained from the Suley man Demirel University Experimental Animal Research Laboratory and housed at 21-22 °C and 60%±5% humidity, with a 12-hour light:12-hour dark cycle. They were fed standard commercial feed ad libitum and provided with water during the experiments. Additionally, Suleyman Demirel University's Scientific

Research Project Unit (SDU-BAP) provided financial support for the study (Project No.: TSG-2024-9515).

Only female rats were used to minimize the confounding influence of androgen-driven vascular responses and to ensure hormonal consistency across groups, given the potential sex differences in endothelial nitric oxide synthesis and BBB permeability.

RF-EMF application

As it is known, 27.12 MHz is located in the part of the ISM Band reserved for Medical Applications. In this study, a quartz crystal oscillator circuit operating at 27.12 MHz, with a power transistor amplifier amplifying the oscillator output, was used. The high-frequency electromagnetic field was designed for homogeneous exposure by ensuring that the exposure was uniform at ever point and that the animals could move freely in the plexigla's cages (EuroType-2) where they were placed. In a ldition, considering the wavelength at the propaga on irequency (11 m), each point of the cage exposure levice is within the near-field region of the source, so a near-field probe can be suitable for observing the noque cy used as an antenna at every stage of the experiments and measurements. As is known, the wavelength for this frequency is approximately 11 meters, and the near-field and far-field limits are 1.75 meters. In other wo. 4s, all experiments have been conducted in the near feld region. The electric field value was targeted as 0 V/m. This value was easily obtained with an additional ti. stor oscillator within acceptable limits (Figure 1).

The shielding efficiency of the electromagnetic isolation room (Faraday Cage) in the laboratory was determined to be 80 dB. For the working frequency of 27.12 MHz, and to minimize the interference effects of possible repetitive reflections in the environment, spectrum analyzers (ROHDE-SCHWARZ FSH6, USA, and PROMAX AE-566 spectrum analyzer, USA) were used. RF-EMF measurements were conducted using a field meter (Mustool MT-525, China), an ELF meter (PF-4, UK), and an Extech 480836 (USA). The targeted 10 V/m electric field value for RF-EMF propagation was produced by the single-transistor oscillator we made as a custom design. The circuit design and antenna structure used in the RF-EMF setup are presented in Supplementary Figure 2.

As shown in Figure 2, the single-transistor oscillator also supplies energy to the antenna, serving as the applicator,

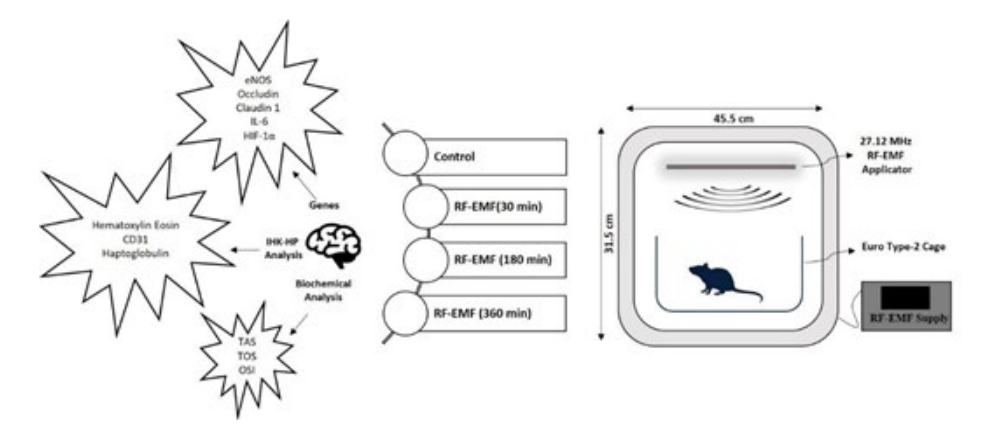


Figure 1. Study design and RF-EMF (27.12 MHz) exposure setup for Wistar Albino rats RF-EMF: Radiofrequency electromagnetic field, IL-6: Interleukin-6, HIF-1α: Hypoxia inducible factor-1 alpha, eNOS: Endothelial nitric oxide synthase, Total oxidant status, TAS: Total antioxidant status, OSI: Oxidative stress index, IHK: Immunohistochemical, HP: Histopathological

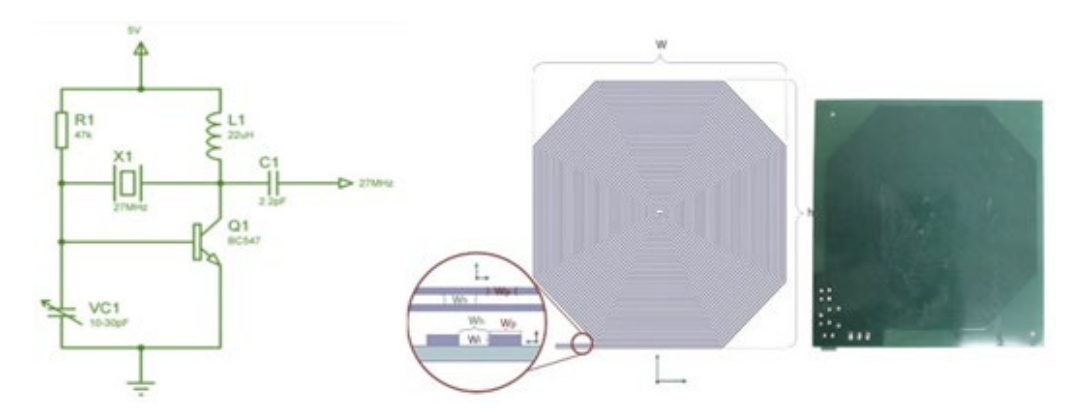


Figure 2. Circuit diagram and 27.12 MHz RF-EMF application antenna used for Wistar Albino rat exposure Octagonal geometry is appropriate for using the PCB antenna as an applicator in the operating frequency

and functions as a power amplifier. Since the circuit is connected directly to the antenna, with no antenna cable in between, the losses are minimal. In this case, two RF-EMF applicators, used 15 cm above the animal cages, provide approximately homogeneous RF-EMF radiation within the cage. An EMF meter was used to measure both the homogeneity within the cage and the obtained electric field value (EXTECH, EMF meter, FLIR Systems, Inc., USA)

The exposure durations (30, 180, and 360 min) were selected based on preliminary studies suggesting time-dependent nitric oxide dynamics and to evaluate both acute and prolonged RF-EMF effects on BBB physiology. The 30-minute duration was chosen in line with prior studies reporting peak eNOS activation at this interval (14), while longer durations aimed to explore cumulative or potentially adverse effects."

Experimental procedure

A total of 24 rats were divided into four groups after being obtained from Suleyman Demirel University Experimental Animal Laboratory. Groups were;

Group 1 (Control)(n=6): Rats were kept under the s. me conditions as the others, but there was no RF-EMF application. After 360 min (the longest RF-EMF application), the rats were euthanized.

Group 2 (30 min exposure)(n = 6): Rats were 'xposed to RF-EMF for 30 min in the unit and then eath. 'ize λ '.

Group 3 (180 min exposure)(n=3): Rats were exposed to RF-EMF for 180 min in the unit; nd then eumanized.

Group 4 (360 min exposure)(n 5): Rats were exposed to RF-EMF for 360 min in the unit and the enthanized.

At the end of these applications, 90 mg/kg ketamine (Keta-Control, Doga Ilac, Turkey) and 8-10 mg/kg xylazine (Xylazinbio, Bioveta, Czech Republic) were given to animals and euthanized by the surgical exsanguination method following abdominal incision. The right hemispheres of the brain and cerebellum tissues were removed following the decapitation procedure and put into 10% formaldehyde for histopathological examination with hematoxylin-eosin staining and immunohistochemical analysis (CD31 and haptoglobin expressions) to examine tissue damage and increased permeability. The levels of the oxidative stress markers total antioxidant species (TAS), total oxidant status (TOS), oxidative stress index (OSI) biochemically, and the expressions of interleukin-6 (IL-6), hypoxia inducible factor-1 alpha (HIF-1a), endothelial nitric oxide synthase

(eNOS), claudin-1, and occludin were investigated with RT-qPCR.

From each group (n=6), three animals were allocated for histopathological and immunohistochemical analyses, while the remaining three were used for biochemical and genetic analyses (RT-qPCR, TAS, TOS, and OSI). This distribution ensured sufficient sissue availability for each method without compromising analytical integrity.

Measurement of oxid....''e ss parameters in the brain tissue

Brain tissues of rate were homogenized with the Ultra Turrax Jorke & Kankel T-25 homogenizer (IKA* Werke, Germany) in 1:9 (w/v) phosphate-buffered saline (10 mM Na*HPO4, 1. mM KH2PO4, 2.7 mM KCl, 137 mM NaCl, pH7*). After that, homogenized liver tissues were analyzed spectrop otometrically for TAS, TOS, and OSI values, as percentaged by Savran et al. (16). The TAS and TOS results in the serum were expressed in µmol Trolox Eq/L and µmol H2O2 Eq/L, respectively. The TAS and TOS results for the tissues were expressed as the ratio of these values to the protein value (17). The OSI was calculated using the formula OSI (TOS/TAS) x 10 (18). Protein levels of the supernatants were determined with a Beckman Coulter autoanalyzer (Beckman Coulter, USA).

TAS levels reflect the cumulative antioxidant capacity of tissue, while TOS represents the total pro-oxidant burden. The OSI index, calculated as TOS/TAS×10, serves as a global indicator of oxidative stress status. All measurements were performed in duplicate using an automated colorimetric method developed by Erel (2004, 2005)(17, 18).

Histopathological evaluation

During the necropsy, samples of the brain and cerebellum were carefully removed and preserved in 10% buffered formalin for histological analysis. After routinely processing the tissues, five-micrometer-thick sections of the paraffin blocks were cut using a rotary microtome (Leica RM2155, Leica Microsystems, Wetzlar, Germany). After deparaffinization, rehydration with ethanol of decreasing concentrations, staining with hematoxylin-eosin (HE), cleaning in xylene, and covering the sections, they were examined under a light microscope. Histological sections were evaluated at ×200 and ×400 magnifications using an Olympus BX53 microscope. Cortical and cerebellar regions were examined explicitly for vascular changes, edema, and



neuronal damage. At the histopathological examination of the brain and cerebellum, hyperemia, hemorrhage, edema, gliosis, and neuronal damage were evaluated.

All histopathological and immunohistochemical evaluations were performed in a blinded manner by two independent observers, who were unaware of the group allocations, to minimize observer bias.

Immunohistochemical examinations

Sections collected onto polylysine-coated slides were immunostained for haptoglobin (Anti-Haptoglobin [EPR22856-212](ab256454),1/100 and CD31 (Anti-CD31 antibody [EPR17259](ab182981), 1/100 dilution) using the streptavidin-biotin technique. Both primary and secondary antibodies were purchased from Abcam (Cambridge, UK). Following a 60-minute incubation period with primary antibodies, sections were immunohistochemically stained using biotinylated secondary antibodies and streptavidin-alkaline phosphatase conjugate. EXPOSE Mouse and Rabbit Specific HRP/DAB Detection IHC kit -ab80436 was used as the secondary antibody, and diaminobenzidine served as the chromogen (DAB). For the negative controls, the primary antiserum phase was replaced with the antigen dilution solution. Blinded samples were used for all tests. The Database Manual Cell Sens Life Science Imaging Software System (Olympus Co., Tokyo, Japan) was used for microphotography at 3 morphometric analysis.

All antibodies used (Abcam) were validated for rat issue cross-reactivity and immunohistochemical specificity the manufacturer. Negative control experiments confirmed the specificity of staining.

Immunoreactive areas were somi-quintitatively evaluated using ImageJ software. Immunipositivity was expressed as a percentage of positively standed area per total field. At least five random fields per somion were analyzed at ×400 magnification.

Reverse transcription-polymerase chain reaction (RT-qPCR)

Using the manufacturer's protocol, RNA was isolated from homogenized tissues with the GeneAll RiboEx (TM) RNA Isolation Kit (GeneAll Biotechnology, Seoul, Korea). The amount and purity of the RNAs obtained were measured using the BioSpec-nano nanodrop device (Shimadzu Ltd.,

Kyoto, Japan). 1 µg RNA was used for cDNA synthesis. cDNA synthesis was performed using the A.B.T. ™ cDNA Synthesis Kit (Atlas Biotechnology, Turkey) in a thermal cycler according to the manufacturer's protocol. Primer designs were made by detecting specific mRNA sequences and testing possible primer sequences using the NCBI website. The sequences of the primers used are shown in Table 1. Expression levels of genes were measured in a Biorad CFX96 (California/USA) real-time PCR instrument using A.B.T.™ cDNA Synthesis Kit (Atlas Biotechnology/ Turkey). In the study, the GAPDH gene was used as a housekeeping gene. The reaction mixture was prepared according to the manufacturers protocol to a final volume of 20 µl. The resulting reaction mixture we placed in a real-time qPCR device, with thermal cycling perlirmed according to the kit manufacturers protocol. Each sample was analyzed in three replicates. PCR condition initial denaturation at 95 °C for 300 sec. 1 cycle, den atura, ion at 95 °C 15 sec., and annealing/ extension at 56 °C 30 °C, were applied to 40 cycles. Relative mRNA Level, were calculated by applying the $2^{-\Delta\Delta Ct}$ formula to the no. maized results.

Star'stical analysis

The results were analyzed for normality distribution, one since all data were normally distributed, one-way ANOVA was used, followed by Tukey's multiple comparison ast. Statistical analysis was performed using GraphPad Prism version 8.0 software (San Diego, California, USA). Differences were considered significant for *P*<0.05. All results are expressed as mean±SD.

Results

Oxidative stress markers

When the oxidative stress parameters were analyzed, no statistical significance was found between the groups for any of the parameters. It was found that RF-EMF application did not trigger oxidative stress in brain tissue during the application of RF-EMF at three different times (Figure 3).

Histopathological findings

During the microscopical examination of the brains and cerebellums, there were no lesions in the control group. The other groups showed slight hyperemia and edema related to the dosage of the exposure (Figure 4).

Table 1. Primary sequences, product size, and accession numbers of genes analyzed in Wistar Albino rats

Genes	Primary sequence	Product size	Accession number
eNOS	F: GGTTGACCAAGGCAAACCAC	247 bp	NM_021838.2
	R: CCTAATACCACAGCCGGAGG		
Occludin	F: TCACTGTGTGACCTGTCTTGG	217 bp	NM_031329.3
	R: ACTGGGCTGGATGCCAATTT		
Claudin 1	F: ACTGTGGATGTCCTGCGTTT	127 bp	NM_031699.3
	R: CCCCAGCAGGATGCCAATTA		
IL-6	F: CACAAGTCCGGAGAGGAGAC	168 bp	NM_012589.2
	R: ACAGTGCATCATCGCTGTTC		
HIF-1α	F: GCAACTAGGAACCGAACCA	251 bp	NM_024359.2
	R: TCGACGTTCGGAACTCATCC		
GAPDH (Housekeeping)	F: AGGTTGTCTCCTGTGACTTC	130 bp	NM_017008.4
	R: CTGTTGCTGTAGCCATATTC		

F: Forward, R: Reverse, GAPDH: glyceraldehyde-3-phosphate dehydrogenase, IL-6: Interleukin-6, HIF-1a: Hypoxia inducible factor-1 alpha, eNOS: Endothelial nitric oxide synthase

Oxidative stress markers

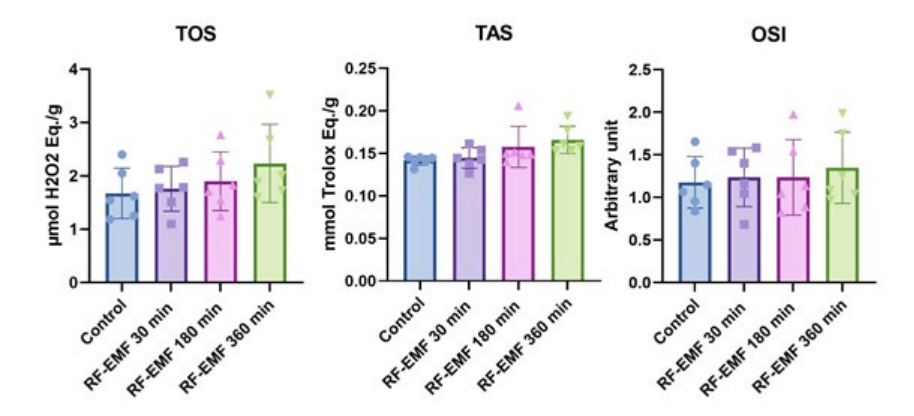


Figure 3. Oxidative stress parameters in Wistar Albino rat brain tissue

Data presented as the mean±standard deviation. The oxidative stress markers were compared between groups using one-way ANOVA (*post-hoc* Tukey's test). *P<0.05; **P<0.01; ***P<0.001

RF-EMF: Radiofrequency electromagnetic field, TOS: Total oxidant status, TAS: Total antioxidant status, OSI: Oxidative stress index

Immunohistochemical findings

At the examination of haptoglobin immunostained slides, only slight expressions were noticed in the cerebellums in the 180-minute and 360-minute exposure groups. No expression was noticed in the other groups (Figures 5, 6).

CD31 immunohistochemical findings revealed negative expressions in the brains in all groups, while slight expressions were observed in the cerebellums. There were no differences between the groups.

RT-qPCR results

No significant difference was observed between groups in terms of IL-6 levels, which is both an acute phase reactant and an activator of the IL-6/HIF- 1α /eNOS pathway. Although IL-6 expression did not reach statistical significance, a slight upward trend was observed at 360 min exposure, potentially indicating a subthreshold inflammatory activation. When

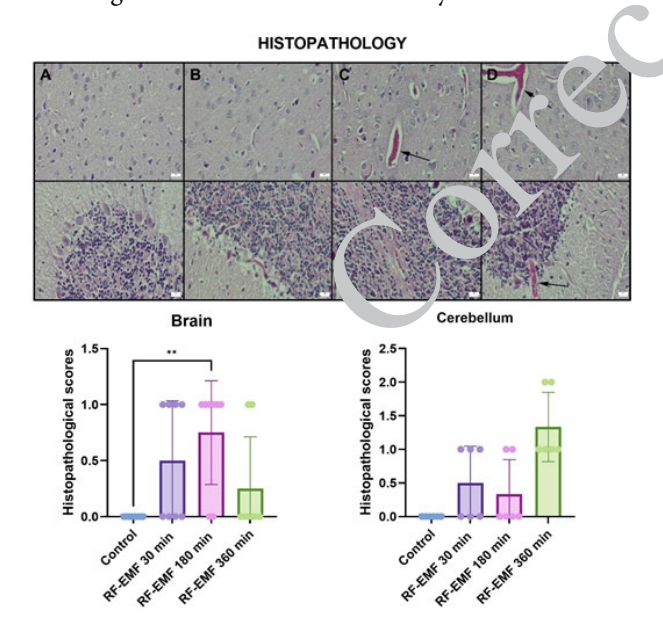


Figure 4. Representative histological sections of the cerebral cortex (upper row) and cerebellum (lower row) from Wistar Albino rats, stained with H&E

(A) Normal architecture in the control group. (B) No marked change in 30-min RF-EMF group. (C) Moderate hyperemia in the 180-min group (arrow). (D) Severe hyperemia and edema in the 360-min group (arrows). Scale bars=50 μ m

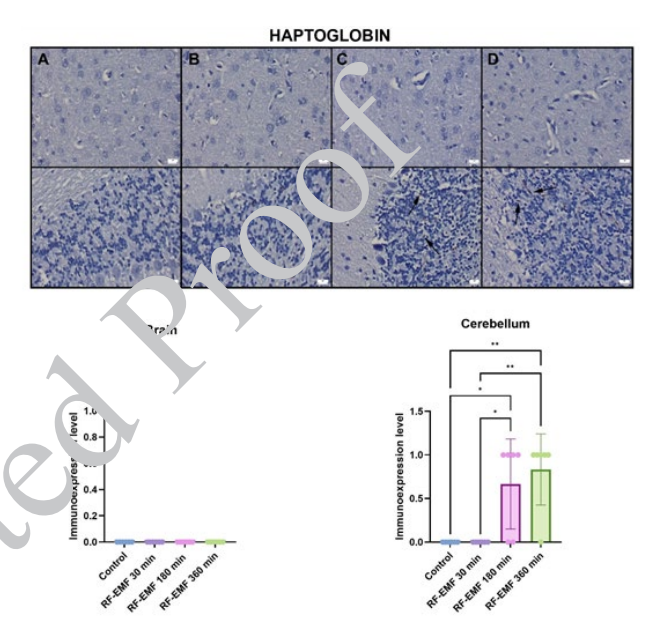


Figure 5. Haptoglobin immunostaining in the cerebral cortex (upper row) and cerebellum (lower row) of Wistar Albino rats (A) No staining in the control. (B) Negative in a 30-minute group. (C) Slight positivity in the cerebellum of the 180-min group (arrow). (D) Slight positivity in 360-min group cerebellum (arrow). Scale bars=50 µm. IHC analysis used the streptavidin-biotin DAB protocol. * P < 0.05; ** P < 0.01; *** P < 0.001

HIF-1 α levels were examined, it was determined that RF-EMF applied for 360 min increased more than the 30-minute group. The NO-producing enzyme eNOS expression was highest in the RF-EMF 30 min (P<0.01) group and increased significantly compared to the control group. While eNOS levels were found to be significantly decreased compared to the RF-EMF 30 min group, a significant difference was detected between these two groups (P<0.05)(Figure 7).

When claudin-1 and occludin levels, which are indicators of BBB permeability, are examined, claudin-1 expression decreased in all three groups. In comparison, it was found to be significant in the RF-EMF 180 min and RF-EMF 360 min groups (P<0.01 for both). Occludin levels were found to be statistically decreased in all three groups compared to the control group (P<0.001 for all)(Figure 8).

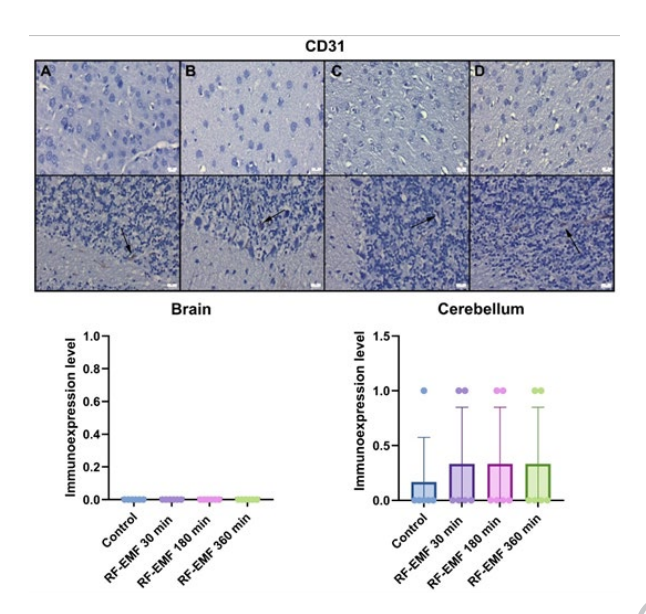


Figure 6. CD31 immunoreactivity in the cerebral cortex (upper row) and cerebellum (lower row) of Wistar Albinc rats (A) Control, (B) 30-min, (C) 180-min, (D) 360-min exposure. No immunostaining observed in cerebral cortex; minimal exposure. in cerebellar vessels in all groups (arrows). Scale bars=50 μm. * P<0.05; ** P<0.01; *** P<0.001

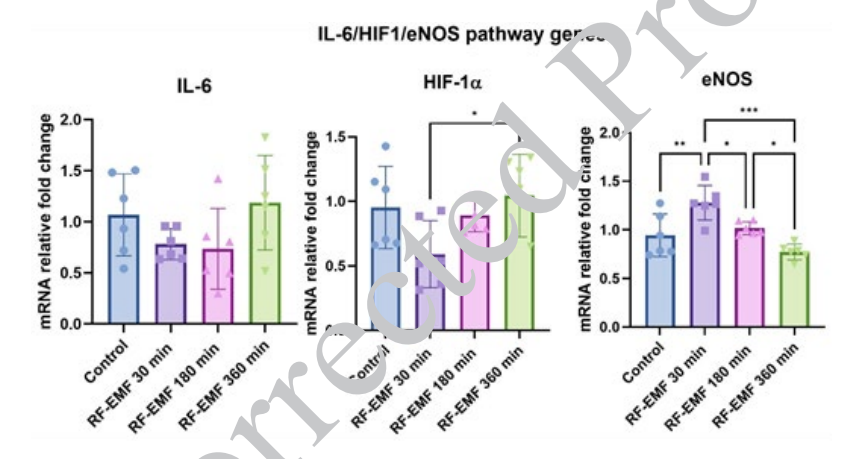


Figure 7. Relative mRNA expression levels of IL 6, HI1 1α, and eNOS in the brain tissue of Wistar Albino rats
Data are mean±SD (n=3/group). eNOS expression sign. feantly increased in the 30-min RF-EMF group compared to the control. One-way ANOVA followed by Tukey's test.
*P<0.05, **P<0.01, ***P<0.001

TIGHT JUNCTION PROTEINS

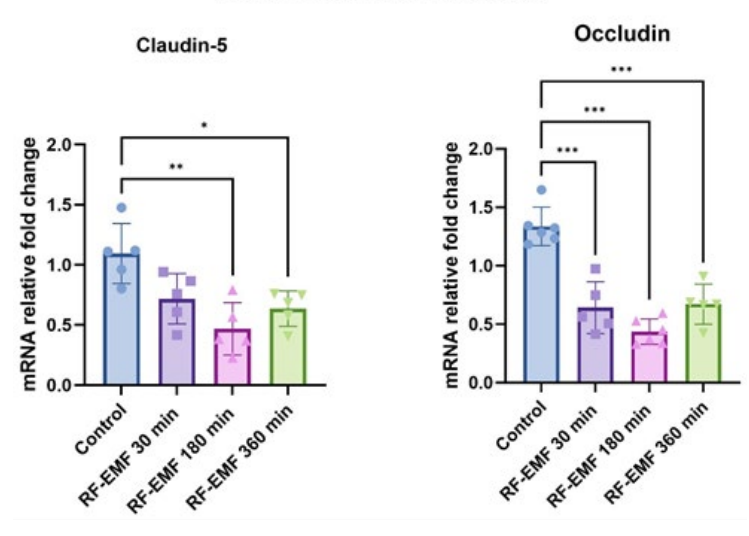


Figure 8. Relative mRNA expression levels of tight junction proteins claudin-1 and occludin in the brain tissue of Wistar Albino rats Claudin-1 significantly decreased in 180- and 360-min groups, while occludin expression was reduced across all RF-EMF exposure durations. Data are presented as mean±SD (n=3). *P<0.05, **P<0.01, ***P<0.001



Discussion

The BBB serves as a dynamic and selective interface that protects the CNS from harmful agents while maintaining homeostasis. However, this protective role can become a therapeutic obstacle in diseases requiring drug penetration into the brain parenchyma. Therefore, the ability to transiently and non-invasively modulate BBB permeability has attracted increasing scientific attention (19). In this context, the present study demonstrates that acute exposure to a 27.12 MHz RF-EMF for 30 min significantly modulates BBB permeability by up-regulating eNOS expression and down-regulating occludin, without inducing inflammation or oxidative stress.

In our experimental setup, 30-, 180-, and 360-minute exposures were selected to explore the temporal dynamics of BBB modulation. Our results clearly show that 30-minute RF-EMF exposure leads to a significant increase in eNOS expression. This finding aligns with prior evidence suggesting that RF-EMF enhances endothelial function and tissue perfusion through NO-dependent pathways (14). Notably, no histological damage or inflammation was observed in this group, suggesting that short-term RF-EMF can transiently open the BBB in a safe and controlled manner.

In contrast, the 180- and 360-minute RF-EMF exposures induced histopathological changes such as hyperemia and edema, particularly in cerebellar tissues, indicating a possible inflammatory response. Although IL-6 expression did not reach statistical significance, its upward trend in the 360-minute group supports the presence of low-grade inflammation. Moreover, HIF-1 α expression was significantly elevated with increasing exposure duration, reflecting hypoxic stress or reactive metabolic compensation. These findings suggest that while longer RF-EMF exposures can further disrupt BBB integrity, they may do so at the cost of tissue stress and vascular reactivity.

Interestingly, eNOS expression declined in the 150- and 360-minute groups, contrary to the 30-minute result One plausible explanation is the depletion of L-rg pine, the substrate for NO synthesis. Previous studies have shown that prolonged NO synthesis can deplete intracellurary arginine pools, particularly under conditions of metabolic stress or inflammation (11). This substrate-linearing mechanism might explain the biphasic eN S response observed here. Nevertheless, this hypothesis a point speculative and warrants future biochemical validation through arginine quantification or eNOS activity assays.

The tight junction proteins claudin-1 and occludin are fundamental to maintaining BBB integrity. Their down-regulation in the 180- and 360-minute groups aligns with the observed histological findings, suggesting a structural compromise of the barrier. Notably, occludin levels were significantly reduced in all exposure groups, including the 30-minute group. While occludin down-regulation typically indicates increased permeability, the absence of inflammatory or oxidative markers in this group implies that the effect may be reversible and functionally selective. This supports the potential of 30-minute RF-EMF exposure as a therapeutic window for transient BBB opening.

The expression of CD31, a marker of endothelial junction stability and vascular remodeling, remained unchanged across all groups, except for minimal expression in cerebellar tissues. This suggests that RF-EMF-induced BBB

modulation does not involve angiogenesis or endothelial proliferation, at least within the exposure durations tested. Similarly, haptoglobin expression, a marker of hemorrhagic stress, was only minimally increased in long-duration groups and absent in 30-minute exposure, further indicating the non-damaging nature of short-term RF-EMF.

Oxidative stress analysis revealed stable TAS, TOS, and OSI levels across all groups, reinforcing the conclusion that RF-EMF, particularly at shorter durations, does not provoke redox imbalance. This contrasts with many other BBB modulation techniques, such as focused ultrasound, which are associated with transient oxidative bursts or microbubble-induced damage (20). Therefore, RF-EMF appears to offer a safer profile for clinical translation, especially in protocols requiring repeated applications.

Compared to focused ultrasound or pulsed magnetic fields, RF-EMF at 27.12 MHz presents advantages such as field uniformity, deeper tissue penetration, and minimal thermal effects at low power densities. Furthermore, unlike pharmacological BBB disruptors (e.g., mannitol or bradykinin analogs), RF-EMF does not induce systemic hypotension or osmotic shifts. These properties make it particularly attractive for lo alized, on-demand BBB modulation in conditions have brain tumors, epilepsy, or CNS infections.

Despite these pronding findings, certain limitations should be a knowledged. The exclusive use of female rats may limit generalizability due to known sex-related differences in endothelial anction and BBB response. Additionally, the relatively small sample size and lack of functional assays (e.g., Eval's blue permeability or tracer imaging) prevent direct quantification of BBB leakage. Future studies should neorporate both sexes, larger cohorts, and functional preschild assays to comprehensively validate the effects of RF-EMF.

Moreover, the absence of long-term follow-up prevents us from assessing the reversibility of BBB opening or potential delayed tissue damage. Investigating whether the BBB reseals within hours or days post-exposure would be essential before clinical translation. The integration of drug delivery trials combining RF-EMF exposure with chemotherapeutics or neuroprotectants would also reveal the functional utility of this approach.

In summary, this study reveals that 30-minute exposure to 27.12 MHz RF-EMF significantly enhances BBB permeability via eNOS up-regulation and occludin down-regulation without inducing histological, oxidative, or inflammatory damage. Longer exposures, while further disrupting barrier structure, may introduce tissue stress and should be approached cautiously. These results provide foundational insight into RF-EMF as a non-invasive BBB modulation tool, with significant implications for drug delivery and neurotherapeutic strategies.

Conclusion

In this study, 27.12 MHz RF-EMF exposure for 30 min significantly modulated BBB permeability by up-regulating eNOS and down-regulating occludin, without inducing oxidative or inflammatory damage. Longer exposures (180 and 360 min) caused structural disruption, increased HIF- 1α levels, and minor haptoglobin expression, indicating tissue stress. These results suggest that short-term RF-EMF may offer a safe and effective non-invasive strategy for



transient BBB opening.

However, the study is limited by the use of only female rats, a small sample size, and the absence of functional permeability or long-term follow-up data. Future research should evaluate sex-related responses, reversibility of BBB modulation, and therapeutic co-application with pharmacological agents. Nonetheless, our findings lay essential groundwork for the development of RF-EMF-based BBB targeting technologies in translational neuroscience and drug delivery.

Acknowledgment

The results presented in this paper were part of a student's thesis. The authors thank Suleyman Demirel University Scientific Research Project Unit (SDU-BAP) for providing financial support (Project No: TSG-2024-9515).

Authors' Contributions

A U and H A designed the experiments; A U, H A, R T, MY T, I I, P K, S C, and O O performed the experiments and collected data; A U, H A, P K, and S C discussed the results and strategy; A U and H A supervised, directed, and managed the study; A U and P K approved the final version to be published.

Conflicts of Interest

The authors declare no potential conflicts of interest.

Declaration

We have not utilized any AI tools or technologies in the preparation of this manuscript.

Funding Statement

Suleyman Demirel University Scientific Research Project Unit (SDU-BAP) provided financial support for the study (project no. TSG-2024-9515)

Statement of Ethics

This study protocol was reviewed ar. 'approved by the Committee on Animal Research of Sule man Demirel University, Isparta (Approval No. 26 01.2023/01-129)

Data Availability Staten ent

All relevant data generated regularized during this study are included in this article. Further inquiries can be directed to the corresponding author.

References

- 1. Segarra M, Aburto MR, Acker-Palmer A. Blood-brain barrier dynamics to maintain brain homeostasis. Trends Neurosci 2021; 44: 393-405.
- 2. Wu D, Chen Q, Chen X, Han F, Chen Z, Wang Y. The bloodbrain barrier: Structure, regulation, and drug delivery. Signal Transduct Target Ther 2023; 8: 217-244.

- 3. Terstappen GC, Meyer AH, Bell RD, Zhang W. Strategies for delivering therapeutics across the blood-brain barrier. Nat Rev Drug Discov 2021; 20: 362-383.
- 4. Rizk AA, Plitman E, Senthil P, Venkatraghavan L, Chowdhury T. Effects of anesthetic agents on blood brain barrier integrity: A systematic review. Can J Neurol Sci 2023; 50: 897-904.
- 5. Hashimoto Y, Campbell M. Tight junction modulation at the blood-brain barrier: Current and future perspectives. Biochim Biophys Acta Biomembr 2020; 1862: 183298-183309.
- 6. Lochhead JJ, Yang J, Ronaldson PT, Davis TP. Structure, function, and regulation of the blood-brain barrier tight junction in central nervous system disorders. Front Physiol 2020; 11:914-931.
- 7. Zhao X, Song S, Sun G, Strong R, Zhang J, Grotta JC, Aronowski J. Neuroprotective role of haptoglobin after intracerebral hemorrhage. J Neurosci 2009; 29: 15819-15827.
- 8. Wimmer I, Tietz S, Nishihara H, Deutsch U, Sallusto F, Gosselet F, *et al.* PECAM-1 stabilizes blood-brain barrier integrity and favors paracellular T-cell diapedesis across the blood-brain barrier during neuroinflammation. Front Immunol 2019; 10: 711-728.
- 9. Kalinowska A, Losy J. PECAM-1, a key player in neuroinflammation. Eur J Neuroi 2006; 13: 1284-1290.
- 10. Voirin AC, Chatard M, Bri, "con-Marjollet A, Pepin JL, Perek N, Roche F. Loss of blood-brain barrier integrity in an *in vitro* model subjected to intermitical hypotaia: is reversion possible with a hif-1α pathway inhibitor. Int J. Aol Sci 2023; 24: 5062-5077.
- 11. Yang N, Yang X, T., γ , ' 'Juang Y, Shi W, Li W, et al. Nitric oxide promotes cere ral is hemia/reperfusion injury through upregulating hypo via-in. ' 'c'ole factor1-α-associated inflammation and apo vios. in 1 'ts. Neurosci Lett 2023; 795: 137034.
- 12. The VF, Audys KL. Nitric oxide and blood-brain barrier integrity. A tioxid Redox Signal 2001; 3: 273-278.
- 1. Bushberg, Chou C, Foster K, Kavet R, Maxson D, Tell R, Ziskin M. TEE committee on man and radiation—COMAR technical i form from statement: Health and safety issues concerning experience of the general public to electromagnetic energy from 50 wireless communications networks. Health Physics 2020; 119: ...6-246.
- 14. Bragin DE, Statom GL, Hagberg S, Nemoto EM. Increases in microvascular perfusion and tissue oxygenation via pulsed electromagnetic fields in the healthy rat brain. J Neurosurg 2015; 122: 1239-1247.
- 15. Taner R, Halil A, Uysal D, Sanem A, Ünlü Md, Oğuzoğlu As, et al. The Effects of combination of radiofrequency and pulsed magnetic field on carotid arteria ischemia and reperfusion induced brain injury: A preliminary report. Med J SDÜ 2023; 30: 630-642. 16. Savran M, Asci H, Erzurumlu Y, Ozmen O, Ilhan I, Sirin MC, et al. Theranekron: A novel anti-inflammatory candidate for acetic acid-induced colonic inflammation in rats. Mol Biol Rep 2022; 49: 8753-8760.
- 17. Erel O. A novel automated direct measurement method for total antioxidant capacity using a new generation, more stable ABTS radical cation. Clin Biochem 2004; 37: 277-285.
- 18. Erel O. A new automated colorimetric method for measuring total oxidant status. Clin Biochem 2005; 38: 1103-1111.
- 19. Kadry H, Noorani B, Cucullo L. A blood-brain barrier overview on structure, function, impairment, and biomarkers of integrity. Fluids Barriers CNS 2020; 17: 69-93.
- 20. Konofagou EE, Tung YS, Choi J, Deffieux T, Baseri B, Vlachos F. Ultrasound-induced blood-brain barrier opening. Curr Pharm Biotechnol 2012; 13: 1332-1345.